

# Quantum complexity and topological phases of matter

Pawel Caputa and Sinong Liu

*Faculty of Physics, University of Warsaw, ul. Pasteura 5, 02-093 Warsaw, Poland.*

(Dated: May 20, 2022)

We find that the complexity of quantum many-body states, defined as a spread in the Krylov basis, may serve as a probe that distinguishes topological phases of matter. We illustrate this analytically in one of the representative examples, the Su-Schrieffer-Heeger model. Moreover, in the same setup, we analyze exactly solvable quench protocols where the evolution of the spread complexity shows distinct features depending on the topological vs non-topological phase of the initial state as well as the quench Hamiltonian.

## INTRODUCTION

Recently, the problem of quantifying complexity in quantum systems has been at the center of attention in different branches of physics. To some extent, this interest in complexity was stimulated by the holographic correspondence [1] and puzzles related to the nature of black holes in quantum gravity. Among others, complexity played essential roles in discussions on the firewall [2], fast scrambling near black hole horizons [3–6], quantum chaos [7], and finally the nature of holographic dictionary itself [8].

What makes holography powerful, is the dual description of quantum gravity in terms of a strongly interacting quantum system. This way, the “complexity” of black hole processes can, in principle, be quantified in the dual model and indeed, many recent works advocated for the most useful probe of complexity in (holographic) quantum field theories (QFTs) (see reviews [9, 10]). Even though these explorations are still in a relative early stage, as the dust is starting to settle, we are provided with new, potentially powerful, tools for exploring the complexity frontier of field theories.

One of the interesting directions where complexity measures can be tested and may provide a new looking glass, is the physics of topological phases of matter [11–13]. Indeed, the importance of complexity in topological order was realised early on (see e.g. [14, 15]). On the other hand, applying geometric ideas from holography to topological phases proved fruitful in [16–18] and recently, frameworks for classification of topological phases were suggested as guiding principle for complexity in holography [19]. Clearly, these two subjects may have a lot to learn from each other. Nevertheless, actual studies of state complexity measures in models with topological phases are in their infancy.

So far, only the Nielsen-type approach to complexity [20–22], was tested in a couple of examples [23–25]. Since this framework, tailor-made for computer science, gives rise to numerous ambiguities in many-body physics, such as the choice of gates with their penalties, cost functions etc., it is not surprising that conclusions on whether complexity is sensitive enough differed between [23] and

[24, 25]. Still [24, 25] argued that, with an appropriate choice for the ambiguities, one may detect different phases by discontinuities in Nielsen’s complexity. Based on the above, whether or not complexity is a universal probe correlated with topological phases remains an open question.

In this work we begin filling this gap by analyzing a new measure of state complexity proposed in [26] called *spread complexity* (defined in the next section) in one of the simplest models with topological phases, the Su-Schrieffer-Heeger (SSH) model [27]. This measure is much less ambiguous, relatively straightforward to compute and already proved handy in diagnosing quantum chaos [26]. We first analytically compute the spread complexity of formation of the ground state and find that it is sensitive to the two phases of the model. Next, we test its evolution following quantum quench protocols and find that it also distinguishes the phases even in this non-equilibrium scenario. Our analytical results not only reinforce the spread complexity as a powerful tool but also give a hope for universality in studying topological phases from the perspective of complexity.

This letter is organised as follows. We first briefly review the spread complexity based on the Krylov basis [26]. Next, apply it in the SSH model and evaluate complexity of formation for the ground state. Then, we consider the time evolution of complexity following quantum quench with different SSH Hamiltonians. Finally, we conclude and discuss future directions. Technical details are included in three appendices.

## SPREAD COMPLEXITY OF QUANTUM STATES

We begin with a brief review of the state complexity measure introduced in [26] and the Krylov basis that plays the main role in the computations. Further details and more pedagogical review can be found in [26, 28]. The starting point of our discussion is a general quantum state  $|\Psi(s)\rangle$  related to some initial  $|\Psi_0\rangle$  by a unitary transformation

$$|\Psi(s)\rangle = e^{-iHs} |\Psi_0\rangle. \quad (1)$$

In the quantum computation parlance,  $|\Psi(s)\rangle$  can be referred to as a “target state” related to a “reference state”  $|\Psi_0\rangle$  by a “unitary circuit” with a “circuit Hamiltonian”  $H$ . Parameter  $s$ , usually  $s \in [0, 1]$ , denotes a “circuit time”, can be also taken arbitrary and regarded as the physical time  $t$  (see below).

A useful measure of quantum state complexity can be defined as a spread of  $|\Psi(s)\rangle$  in the Hilbert space (relative to  $|\Psi_0\rangle$ ) [26]. More precisely, the spread complexity of  $|\Psi(s)\rangle$  is estimated by the minimum over all choices of basis  $\mathcal{B} = \{|B_n\rangle, n = 0, 1, 2, \dots | B_0\rangle = |\Psi_0\rangle\}$  of the following cost function

$$\mathcal{C}(s) = \min_{\mathcal{B}} \left( \sum_n n |\langle \Psi(s) | B_n \rangle|^2 \right). \quad (2)$$

The fact that makes this definition powerful and computable is that the minimum is attained (see [26] for proofs) when basis  $\mathcal{B}$  is the so-called Krylov basis that we now review.

The idea behind the Krylov basis for state (1) is to consider states with all the different powers of the circuit Hamiltonian acting on the initial state  $|\Psi_0\rangle$ , i.e.,  $\{|\Psi_0\rangle, H|\Psi_0\rangle, H^2|\Psi_0\rangle, \dots\}$ , and apply the Gram–Schmidt orthogonalization procedure, known as the Lanczos algorithm [29], to this set. In this new basis  $|K_n\rangle$ , the circuit Hamiltonian  $H$  is generally tri-diagonal and acts as

$$H|K_n\rangle = a_n|K_n\rangle + b_n|K_{n-1}\rangle + b_{n+1}|K_{n+1}\rangle, \quad (3)$$

where coefficients  $a_n$  and  $b_n$ , the so-called Lanczos coefficients, can be recursively constructed using the Lanczos algorithm. The information about them is also contained in the moments of the return-amplitude (auto-correlator)  $S(s) \equiv \langle \Psi(s) | \Psi(0) \rangle$ .

Having constructed the basis that minimizes (2), we expand our state as

$$|\Psi(s)\rangle = \sum_n \psi_n(s) |K_n\rangle, \quad (4)$$

where, by construction, the complex coefficients in this expression satisfy a discrete Schrodinger equation

$$i\partial_s \psi_n(s) = a_n \psi_n(s) + b_n \psi_{n-1}(s) + b_{n+1} \psi_{n+1}(s). \quad (5)$$

With the knowledge of the Lanczos coefficients, we can solve it with initial condition  $\psi_n(0) = \delta_{n,0}$  (so that we start from  $|K_0\rangle = |\Psi_0\rangle$ ), and determine (4). Note that unitarity implies that  $\sum_n (p_n(s) \equiv |\psi_n(s)|^2) = 1$ . Moreover, the return amplitude is related to the first coefficient by  $S(s) = \psi_0^*(s)$ . Last but not the least, the number of the independent Krylov vectors depends on the Hamiltonian as well as the initial state  $|\Psi_0\rangle$ .

Most importantly, in the Krylov basis, the complexity (2) becomes

$$\mathcal{C}(s) = \sum_n n |\psi_n(s)|^2, \quad (6)$$

and for all practical purposes, this will be our working definition of the spread complexity in the remaining part of this paper. This measure naturally generalizes the Krylov complexity of operators [30] to quantum states (see e.g. [31] for applications in the SSH model). Among other interesting properties, under time evolution in random matrix theory, spread complexity exhibits universal features analogous to the spectral form factor [32] that make it a promising candidate for a probe of quantum chaos. In the following, we will employ (6) and test whether it does equally well in integrable systems and in particular, whether it can detect topological phases.

## SPREAD COMPLEXITY IN THE SSH MODEL

Our basic example will be the SSH model of polyacetylene [27] (see e.g. [33] for a pedagogical introduction, here we closely follow the conventions of [34, 35]) given by the Hamiltonian

$$H = t_1 \sum_i \left( c_{Ai}^\dagger c_{Bi} + \text{h.c.} \right) - t_2 \sum_i \left( c_{Bi}^\dagger c_{A,i+1} + \text{h.c.} \right) + \mu_s \sum_i \left( c_{Ai}^\dagger c_{Ai} - c_{Bi}^\dagger c_{Bi} \right), \quad (7)$$

where  $(c_{Ai}, c_{Bi})$  represent two-flavours of fermion annihilation operators defined at site  $i$  on a 1d lattice, and  $t_1, t_2, \mu_s$  are real parameters. We will assume  $t_1 \geq 0$  and  $t_2 \geq 0$  and  $\mu_s = 0$ . Depending on these couplings, the model is in one of the two phases: a non-topological phase for  $t_1 > t_2$  or a topological phase (topological insulator) for  $t_2 > t_1$ , separated by a critical point at  $t_1 = t_2$ .

We will first compute the complexity of the ground state that, depending on parameters  $t_1$  and  $t_2$ , belongs to one of the above-mentioned phases of the model. Strictly speaking, we should call it the spread complexity of formation of the ground-state and it is a slight generalisation of the definition for real time  $t$  in [26]. Nevertheless, since the main step in computing the spread complexity is to rewrite the ground-state as a quantum circuit (1), the framework works equally well for the circuit time  $s$ .

For that, as well as for later purposes, it will be convenient to re-write the Hamiltonian in momentum space as (see [35], and appendix A)

$$H = \sum_k \left[ 2R_3 J_0^{(k)} + iR_1 \left( J_+^{(k)} - J_-^{(k)} \right) \right], \quad (8)$$

where the coefficients are  $R_1 = t_1 - t_2 \cos(k)$ ,  $R_3 = t_2 \sin(k)$  and, for each momentum mode, we denoted the  $SU(2)$  algebra generators

$$[J_0^{(k)}, J_\pm^{(k)}] = \pm J_\pm^{(k)}, \quad [J_+^{(k)}, J_-^{(k)}] = 2J_0^{(k)}. \quad (9)$$

Then, the ground state can be written in terms of the

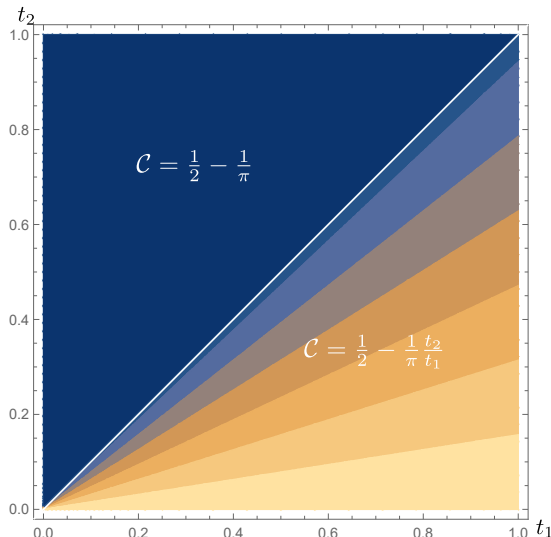


FIG. 1. Behaviour of the spread complexity of formation  $\mathcal{C}(t_1, t_2)$  (equation (16)) for the ground state of the SSH model  $|\Omega\rangle$ .

$SU(2)$  coherent states as

$$|\Omega\rangle = \prod_{k>0} \mathcal{N}_k e^{-i \tan\left(\frac{\phi_k}{2}\right)(J_+^{(k)} + J_+^{(-k)})} \left| \frac{1}{2}, -\frac{1}{2} \right\rangle_k, \quad (10)$$

where  $\mathcal{N}_k$  stands for the normalization,  $J^{(\pm k)}$  correspond to two decoupled  $SU(2)$  algebras for positive and negative momenta and  $|1/2, -1/2\rangle$  denotes a tensor product over the lowest-weight states of the  $j = 1/2$  representation ( $J_-^{(\pm k)} |1/2, -1/2\rangle_{\pm k} = 0$ ). Moreover, the relation between  $\phi_k$  and the physical parameters is given by

$$\sin \phi_k = \frac{|R_1|}{R}, \quad \cos \phi_k = \frac{R_3}{R}, \quad (11)$$

where we also denoted

$$R = \sqrt{t_1^2 + t_2^2 - 2t_1 t_2 \cos(k)}. \quad (12)$$

Without loss of generality, we can just compute the spread complexity for positive momenta and the full result will have an additional factor of 2 from the  $-k$  sector.

First, for a single momentum  $k > 0$ , using the  $SU(2)$  Baker–Campbell–Hausdorff formula and with a slight abuse of notation, we write the relevant part of the state in a circuit form (1)

$$|\Omega_k(s)\rangle = e^{-i \frac{s\phi_k}{2} (J_+^{(k)} + J_-^{(k)})} \left| \frac{1}{2}, -\frac{1}{2} \right\rangle_k, \quad (13)$$

where  $s \in [0, 1]$  and our ground state is the “target state” at  $s = 1$ . Note that in these circuits we took a natural reference state as the ground state of the left and right Hamiltonians (see appendix A). This way of writing makes transparent the connection with coherent states

and we can directly apply the tools from [28] (see appendix B) to expand our state in the Krylov basis as (4). Because  $j = 1/2$ , we will only have two basis vectors and two amplitudes

$$\psi_0(s) = \cos\left(\frac{s\phi_k}{2}\right), \quad \psi_1(s) = -i \sin\left(\frac{s\phi_k}{2}\right), \quad (14)$$

that satisfy (5) with appropriate Lanczos coefficients. As a result, we get the contribution to our complexity from a single momentum mode

$$\mathcal{C}_k(s=1) = \sin^2 \frac{\phi_k}{2} = \frac{1}{2} - \frac{t_2 \sin(k)}{2\sqrt{t_1^2 + t_2^2 - 2t_1 t_2 \cos(k)}}. \quad (15)$$

The complexity of the ground state is obtained by integrating over all the momenta and multiplying by 2 from  $k < 0$ . This yields

$$\mathcal{C}(t_1, t_2) = 2 \int_0^\pi \frac{dk}{2\pi} \mathcal{C}_k = \frac{1}{2} - \frac{t_1 + t_2 - |t_1 - t_2|}{2\pi t_1}. \quad (16)$$

Observe that we took the continuum limit so this result is proportional to the volume  $L$  but, to keep our equations compact, we rescaled this factor (our  $\mathcal{C}$  are complexity “densities”).

This surprisingly simple formula, shown on Fig. 1, indeed shows two very different behaviours of the spread complexity for the two distinct phases of the model. Namely, for the non-topological phase with  $t_1 > t_2$ , complexity linearly depends on the ratio  $t_2/t_1$  but in the topological phase, with  $t_2 > t_1$ , it is constant. This is one of our main results. We also performed analogous computation for the 1d Kitaev-chain [36], and found that complexity becomes constant when crossing from a non-topological to a topological phase in specific cases [37]. Note that unlike entanglement entropy or Nielsen-type complexities that require numerics, (16) is fully analytical.

## COMPLEXITY DURING QUANTUM QUENCH

Another framework where we can probe the spread complexity is given by the so-called quantum quenches. A typical quench protocol considers a unitary time evolution of an initial state  $|\Omega_i\rangle$  of some initial Hamiltonian  $H_i$ , performed with a different Hamiltonian  $H_f$  for which  $|\Omega_i\rangle$  is an excited state. Universal features of the evolution of entanglement and complexity have been extensively studied in the literature (see e.g. [38–41] and review of closely related dynamical quantum phase transitions [42]).

Here, we focus on the so-called instantaneous quench in the SSH model and consider the state

$$|\Psi(t)\rangle = e^{-iH_f t} |\Omega_i\rangle, \quad (17)$$

where  $|\Omega_i\rangle$  is taken as the ground state of the initial Hamiltonian  $H_i$  with parameters  $(t_1^i, t_2^i)$ , and the evolution is performed with the SSH Hamiltonian  $H_f$  with

different parameters  $(t_1^f, t_2^f)$ . For this state, we will be interested in the Krylov basis and universal features of the real-time evolution of the spread complexity defined above.

Curiously, the Nielsen-type geometric complexity measures for free fields [21] as well as complexity based on the Fubini-Study distance [22], were analyzed during such quenches in the SSH model before [23]. In this work, authors found that above-mentioned complexities were neither sensitive enough to distinguish topological phases nor whether the evolution is driven by  $H_f$  or  $H_i$ . This gives us another strong motivation to test the spread complexity and its sensitivity out of equilibrium.

Similarly to the ground state, since the SSH Hamiltonian consists of the  $SU(2)$  generators (for each momentum mode), we can employ coherent state techniques to expand the quench state (17) in the Krylov basis and find contribution to spread complexity from each mode. This analysis is based on the return amplitude (also known as Loschmidt amplitude) that for each mode  $k > 0$  reads

$$S_k(t) = \langle \Psi(t) | \Psi(0) \rangle = \cos(R_f t) - i \cos(\phi_f - \phi_i) \sin(R_f t). \quad (18)$$

In this formula we used the notation  $R_{i/f}$  that simply stands for (12) with parameters  $(t_1^{i/f}, t_2^{i/f})$  and similarly  $\phi_{i/f}$  are related to the momentum and parameters as in (11) with  $(t_1^{i/f}, t_2^{i/f})$ . From (18) we can repeat the whole procedure to extract Lanczos coefficients, derive  $\psi_n(t)$  and compute spread complexity as before. The contribution from a single momentum mode becomes

$$C_k(t) = \sin^2(\phi_f - \phi_i) \sin^2(R_f t). \quad (19)$$

Clearly, for each mode, complexity is periodic in time with periods governed by the parameters of the evolving Hamiltonian  $H_f$ . The spread complexity is then not symmetric under the change of parameters of initial and final Hamiltonians (as in [23]). The amplitude depends on both, initial and final parameters.

The total complexity is obtained by integrating over the momenta and multiplying by the factor of 2 from negative  $k$ . In the continuum, this can be written in a compact form as an integral (again a density)

$$C(t) = 2 \int_0^\pi \frac{dk}{2\pi} \frac{(t_1^f t_2^i - t_1^i t_2^f)^2 \sin^2(k) \sin^2(R_f t)}{R_f^2 R_i^2}, \quad (20)$$

and for general parameters we need to integrate it numerically. Let us first study some of the analytical examples. Clearly, the spread complexity vanishes if  $t_1^i = t_1^f = 0$  or  $t_2^i = t_2^f = 0$ . Hence, this measure assigns zero costs to evolution of states with Hamiltonians on the axes of the  $t_1-t_2$  plane, as long as they are evolved with Hamiltonian on the same axis (that may have a different parameter  $t_2^{i/f}$  in the first or  $t_1^{i/f}$  in the second family).

A more interesting analytical example is derived if one of

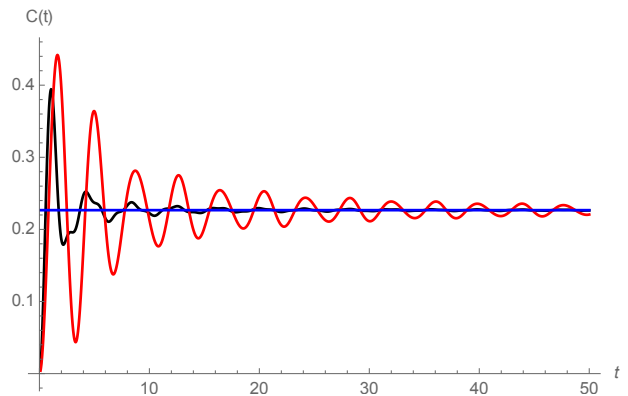


FIG. 2. Evolution of spread complexity starting from  $H_i$  with  $(t_1^i = 1, t_2^i = 0.2)$  and  $(t_1^f = 0.7, t_2^f = 1.5)$  (in black) and the same parameters in  $H_i$  and  $H_f$  switched (in red). At late times complexity approaches constant (23) (in blue).

the parameters of  $H_f$  vanishes i.e.,  $t_{1(2)}^f = 0$ . The total spread complexity is then oscillating with frequency  $t_{2(1)}^f$

$$C(t) = \frac{(t_1^i + t_2^i - |t_1^i - t_2^i|)^2}{8(t_{2(1)}^i)^2} \sin^2(t t_{2(1)}^f), \quad (21)$$

and the amplitude of these oscillations distinguishes the two phases of the initial quench state  $|\Omega_i\rangle$ .

Generally, we can just pick two Hamiltonians, each with a pair of generic parameters in each of the two phases, and compare the evolution of the ground state  $|\Omega_i\rangle$  of  $H_i$  in the topological phase with  $H_f$  in the non-topological phase, and other way around (by just switching parameters  $t_a^i$  with  $t_a^f$  in (20)). This is plotted in Fig. 2 and, unlike Nielsen complexities studied in [23], we can verify that our complexity measure can distinguish the two different quench protocols [43]. This is our second key finding.

In addition, we can derive universal results analytically for the early as well as late time evolution of the spread complexity. For that, it is useful to parametrize  $t_2^i \equiv \alpha t_1^i$  and  $t_2^f \equiv \beta t_1^f$ , such that the topological and non-topological phases are separated by  $\alpha, \beta = 1$ . Then, in the early times we have a universal quadratic growth

$$C(t) \sim (\alpha - \beta)^2 \frac{(1 + \alpha - |1 - \alpha|)^2}{8\alpha^2} (t_1^f)^2 t^2, \quad (22)$$

so this early time regime distinguishes whether  $|\Omega_i\rangle$  is in the topological or non-topological phase.

Also for late times, as it can be observed from Fig. 2, complexity approaches a constant that is given by

$$C(t \rightarrow \infty) = \frac{(\alpha - \beta)}{8\alpha\beta} \times \left( \beta - \alpha + \frac{\alpha(\beta + 1)|\beta - 1| - \beta(\alpha + 1)|\alpha - 1|}{1 - \alpha\beta} \right). \quad (23)$$

Clearly, this constant only depends on the two combinations,  $\alpha$  and  $\beta$ , of the four parameters of the model and is symmetric under their exchange. Therefore, it is the same for both protocols (see Fig. 2) discussed above but it depends on the phases of the model. Note that this constant is the effect of summing of all the, otherwise periodic, contributions from different momenta. We have analyzed it in more detail in appendix C and it is clear that this *spread complexity constant* can be also used as a probe of the late-time physics of the quench state. More detailed studies of this constant in different models with topological phases will be presented in [37].

## CONCLUSIONS AND DISCUSSION

In this letter, we argued that the spread complexity based on the Krylov basis [26] is a sensitive probe of topological phases. We found that, for the ground state of the SSH model, the complexity depends on the ratio of parameters  $t_1/t_2$  in the trivial phase, whereas it becomes constant in the topological insulator regime. Based on other preliminary studies [37], we expect that this behaviour is universal and further tests (including numerics) in more general models will be very important to verify this observation.

For the quantum quench, our main goal was to demonstrate the advantage of the spread complexity over more geometric measures studied in [23]. Not only was this clearly shown but we also found various universal features of the evolution, e.g. at early and late times, that are sensitive to the topological phases. Still, more analysis of the dynamics of spread complexity (e.g. during slow or fast-type quenches, with time-dependent Hamiltonians or Floquet driving) is needed and we leave as a promising future direction. Along the same lines, it will be very interesting to study the spread complexity (and generally Krylov complexity tools) in the context of dynamical quantum phase transitions [42].

Last but not the least, it will be very important to understand the relation between the spread complexity and other topological order parameters already studied in the literature, such as Berry phases or Chern number, that can even be extracted experimentally using certain quench protocols [45]. In fact, there is a striking similarity in the computation of the Krylov or the spread complexity and Berry phases. For example, in [28], it was noted that Krylov complexity is proportional to the volume in the Hilbert space measured using the Fubini-Study metric or, equivalently, to an integral of a certain Berry connection. This link may play an important role in sharpening the spread complexity as a tool in condensed matter physics as well as in the holographic explorations on the complexity frontier of black holes.

**Acknowledgements** We are grateful to Jan Boruch,

Diptarka Das, Sumit Das, Dongsheng Ge, Shajid Haque, Javier Magan, Pratik Nandy, Tokiro Numasawa, Dimitrios Patramanis, Shinsei Ryu and Christof Weitenberg for useful discussions and comments. This work is supported by NAWA “Polish Returns 2019” PPN/PPO/2019/1/00010/U/0001 and NCN Sonata Bis 9 2019/34/E/ST2/00123 grants.

- 
- [1] J. M. Maldacena, “The Large N limit of superconformal field theories and supergravity” Adv. Theor. Math. Phys. **2** (1998) 231 [Int. J. Theor. Phys. **38** (1999) 1113] [arXiv:hep-th/9711200];
  - [2] D. Harlow and P. Hayden, “Quantum Computation vs. Firewalls,” JHEP **06** (2013), 085 [arXiv:1301.4504 [hep-th]].
  - [3] S. Aaronson, “The Complexity of Quantum States and Transformations: From Quantum Money to Black Holes”, [arXiv:1607.05256 [hep-th]].
  - [4] L. Susskind, “Computational Complexity and Black Hole Horizons,” Fortsch. Phys. **64** (2016) 24 [arXiv:1403.5695 [hep-th], arXiv:1402.5674 [hep-th]];
  - [5] D. Stanford and L. Susskind, “Complexity and Shock Wave Geometries,” Phys. Rev. D **90** (2014) no.12, 126007 [arXiv:1406.2678 [hep-th]].
  - [6] A. R. Brown, D. A. Roberts, L. Susskind, B. Swingle and Y. Zhao, “Holographic Complexity Equals Bulk Action?,” Phys. Rev. Lett. **116** (2016) no.19, 191301 [arXiv:1509.07876 [hep-th]].
  - [7] J. Maldacena, S. H. Shenker and D. Stanford, “A bound on chaos,” JHEP **08** (2016), 106 [arXiv:1503.01409 [hep-th]].
  - [8] A. Bouland, B. Fefferman and U. Vazirani, “Computational pseudorandomness, the wormhole growth paradox, and constraints on the AdS/CFT duality,” [arXiv:1910.14646 [quant-ph]].
  - [9] S. Chapman and G. Policastro, “Quantum computational complexity from quantum information to black holes and back,” Eur. Phys. J. C **82** (2022) no.2, 128 [arXiv:2110.14672 [hep-th]].
  - [10] B. Chen, B. Czech and Z. z. Wang, “Quantum information in holographic duality,” Rept. Prog. Phys. **85** (2022) no.4, 046001 [arXiv:2108.09188 [hep-th]].
  - [11] M. Z. Hasan and C. L. Kane, “Topological Insulators,” Rev. Mod. Phys. **82** (2010), 3045 [arXiv:1002.3895 [cond-mat.mes-hall]].
  - [12] X. L. Qi and S. C. Zhang, “Topological insulators and superconductors,” Rev. Mod. Phys. **83** (2011) no.4, 1057-1110 [arXiv:1008.2026 [cond-mat.mes-hall]].
  - [13] A. P. Schnyder, S. Ryu, A. Furusaki, A.W. W. Ludwig “Classification of topological insulators and superconductors in three spatial dimensions” Phys. Rev. B **78**, 195125 (2008)
  - [14] D. Aharonov, L. Eldar, “On the complexity of Commuting Local Hamiltonians, and tight conditions for Topological Order in such systems” [arXiv:1102.0770 [quant-ph]]
  - [15] J. Miller, A. Miyake, “Latent Computational Complexity of Symmetry-Protected Topological Order with Fractional Symmetry” Phys. Rev. Lett. **120**, 170503 (2018) [arXiv:1612.08135 [quant-ph]]

- [16] X. Wen, G. Y. Cho, P. L. S. Lopes, Y. Gu, X. L. Qi and S. Ryu, “Holographic Entanglement Renormalization of Topological Insulators,” *Phys. Rev. B* **94** (2016) no.7, 075124 [arXiv:1605.07199 [cond-mat.mes-hall]].
- [17] M. Aguado and G. Vidal, “Entanglement renormalization and topological order,” *Phys. Rev. Lett.* **100** (2008), 070404 [arXiv:0712.0348 [cond-mat.str-el]].
- [18] S. Matsuura and S. Ryu, “Momentum space metric, non-local operator, and topological insulators,” *Phys. Rev. B* **82** (2010), 245113 [arXiv:1007.2200 [cond-mat.mes-hall]].
- [19] B. Czech, “Holographic State Complexity from Group Cohomology,” [arXiv:2201.01303 [hep-th]].
- [20] M. A. Nielsen, “A geometric approach to quantum lower bounds”, [arXiv:0502070 [quant-ph]].  
M. A. Nielsen, M. R. Dowling, M. Gu and A. C. Doherty “Quantum computation as geometry”, *Science* **311**, 1133 (2006), [arXiv:0603161 [quant-ph]].
- [21] R. Jefferson and R. C. Myers, “Circuit complexity in quantum field theory,” *JHEP* **10** (2017), 107 [arXiv:1707.08570 [hep-th]].
- [22] S. Chapman, M. P. Heller, H. Marrochio and F. Pastawski, “Toward a Definition of Complexity for Quantum Field Theory States,” *Phys. Rev. Lett.* **120** (2018) no.12, 121602 [arXiv:1707.08582 [hep-th]].
- [23] T. Ali, A. Bhattacharyya, S. Shajidul Haque, E. H. Kim and N. Moynihan, “Post-Quench Evolution of Complexity and Entanglement in a Topological System,” *Phys. Rev. Lett.* **811** (2020), 135919 [arXiv:1811.05985 [hep-th]].
- [24] F. Liu, S. Whitsitt, J. B. Curtis, R. Lundgren, P. Titum, Z. C. Yang, J. R. Garrison and A. V. Gorshkov, “Circuit complexity across a topological phase transition,” *Phys. Rev. Res.* **2** (2020) no.1, 013323 [arXiv:1902.10720 [quant-ph]].
- [25] Z. Xiong, D. X. Yao and Z. Yan, “Nonanalyticity of circuit complexity across topological phase transitions,” *Phys. Rev. B* **101** (2020) no.17, 174305 [arXiv:1906.11279 [cond-mat.str-el]].
- [26] V. Balasubramanian, P. Caputa, J. Magan and Q. Wu, “Quantum chaos and the complexity of spread of states,” [arXiv:2202.06957 [hep-th]].
- [27] W. P. Su, J. R. Schrieffer and A. J. Heeger, “Solitons in polyacetylene,” *Phys. Rev. Lett.* **42** (1979), 1698-1701
- [28] P. Caputa, J. M. Magan and D. Patramanis, “Geometry of Krylov complexity,” *Phys. Rev. Res.* **4** (2022) no.1, 013041 [arXiv:2109.03824 [hep-th]].
- [29] C. Lanczos, “An iteration method for the solution of the eigenvalue problem of linear differential and integral operators,” *J. Res. Natl. Bur. Stand. B* **45** (1950), 255-282  
V. Viswanath, G. Müller, “The Recursion Method: Application to Many-Body Dynamics”, vol. 23 Science Business Media
- [30] D. E. Parker, X. Cao, A. Avdoshkin, T. Scaffidi and E. Altman, “A Universal Operator Growth Hypothesis,” *Phys. Rev. X* **9** (2019) no.4, 041017 [arXiv:1812.08657 [cond-mat.stat-mech]].
- [31] D. J. Yates, A. G. Abanov and A. Mitra, “Long-lived period-doubled edge modes of interacting and disorder-free Floquet spin chains,” *Commun. Phys.* **5** (2022), 43 [arXiv:2105.13766 [cond-mat.str-el]].  
D. J. Yates and A. Mitra, “Strong and almost strong modes of Floquet spin chains in Krylov subspaces,” *Phys. Rev. B* **104** (2021) no.19, 195121 [arXiv:2105.13246 [cond-mat.str-el]].
- [32] J. S. Cotler, G. Gur-Ari, M. Hanada, J. Polchinski, P. Saad, S. H. Shenker, D. Stanford, A. Streicher and M. Tezuka, “Black Holes and Random Matrices,” *JHEP* **05** (2017), 118 [erratum: *JHEP* **09** (2018), 002] [arXiv:1611.04650 [hep-th]].
- [33] J.K. Asbóth, L. Oroszlány, A. Pályi, “A short course on topological insulators,” *Lecture notes in physics*, 2016 - Springer
- [34] S. Ryu and Y. Hatsugai, “Entanglement entropy and the Berry phase in the solid state,” *Phys. Rev. B* **73**, 245115 (2006) [arXiv:0601237 [cond-mat.mes-hall]]
- [35] M. Miyaji, S. Ryu, T. Takayanagi and X. Wen, “Boundary States as Holographic Duals of Trivial Spacetimes,” *JHEP* **05** (2015), 152 [arXiv:1412.6226 [hep-th]].
- [36] A. Y. Kitaev, “Unpaired Majorana fermions in quantum wires,” *Phys. Usp.* **44** (2001) no.10S, 131-136 [arXiv:cond-mat/0010440 [cond-mat.mes-hall]].
- [37] P. Caputa, S. Liu, work in progress
- [38] A. Mitra, “Quantum quench dynamics”, *Annual Review of Condensed Matter Physics*, Vol. 9:245-259 (2018) [arXiv:1703.09740 [cond-mat.quant-gas]]
- [39] P. Calabrese and J. Cardy, “Quantum quenches in 1 + 1 dimensional conformal field theories,” *J. Stat. Mech.* **1606** (2016) no.6, 064003 [arXiv:1603.02889 [cond-mat.stat-mech]].
- [40] H. A. Camargo, P. Caputa, D. Das, M. P. Heller and R. Jefferson, “Complexity as a novel probe of quantum quenches: universal scalings and purifications,” *Phys. Rev. Lett.* **122** (2019) no.8, 081601 [arXiv:1807.07075 [hep-th]].
- [41] S. Liu, “Complexity and scaling in quantum quench in 1+1 dimensional fermionic field theories,” *JHEP* **07** (2019), 104 [arXiv:1902.02945 [hep-th]].
- [42] M. Heyl, “Dynamical quantum phase transitions: a review,” *Rept. Prog. Phys.* **81** (2018) no.5, 054001 [arXiv:1709.07461 [cond-mat.stat-mech]].
- [43] Since the analysis in [23] was numerical and mostly focused on late times, it may still be possible that a more careful study of this quenches (along the lines of [44]) at early times will allow to distinguish the two setups. We thank Shajid Haque for his feedback.
- [44] T. Ali, A. Bhattacharyya, S. Shajidul Haque, E. H. Kim and N. Moynihan, “Time Evolution of Complexity: A Critique of Three Methods,” *JHEP* **04** (2019), 087 [arXiv:1810.02734 [hep-th]].
- [45] Tarnowski, M., Únal, F.N., Fläschner, N. et al. , “Measuring topology from dynamics by obtaining the Chern number from a linking number.” *Nat Commun* **10**, 1728 (2019).
- [46] A. M. Perelomov, “Coherent states for arbitrary Lie group”, *Commun. Math. Phys.* **26** (1972) 222.
- [47] J.P. Gazeau, “Coherent States in Quantum Physics”, 2009, Wiley

## Appendix A: Details on SSH

In this appendix we explain some of the details of the SSH model and few steps to express it in the language of  $SU(2)$  coherent states.

First, via a Fourier transformation

$$\begin{pmatrix} c_{Al} \\ c_{Bl} \end{pmatrix} = N^{-1/2} \sum_{k \in \text{BZ}} e^{ikl} \begin{pmatrix} \tilde{c}_k \\ \tilde{d}_k \end{pmatrix}, \quad (24)$$

and a rotation of Pauli matrices  $(\sigma_x, \sigma_y, \sigma_z) \rightarrow (\sigma_x, \sigma_z, -\sigma_y)$ , the Hamiltonian in position space (7) turns into a free fermion one in momentum space

$$H = \sum_{k \in \text{BZ}} \Psi_k^\dagger \vec{R}(k) \cdot \vec{\sigma} \Psi_k, \quad \Psi_k = \begin{pmatrix} c_k \\ d_k \end{pmatrix} = e^{-\frac{i\pi}{4} \sigma_x} \begin{pmatrix} \tilde{c}_k \\ \tilde{d}_k \end{pmatrix}, \quad (25)$$

where the vector of parameters reads

$$\vec{R}(k) = \begin{pmatrix} R_1 \\ R_2 \\ R_3 \end{pmatrix} = \begin{pmatrix} t_1 - t_2 \cos k \\ -\mu_s \\ t_2 \sin k \end{pmatrix}.$$

The Hamiltonian (25) can be further diagonalised into

$$H = \sum_{k \in \text{BZ}} \chi_k^\dagger \text{diag}(R, -R)(k) \chi_k, \quad (26)$$

where we write the norm  $R(k) = |\vec{R}(k)|$ , and

$$\chi_k = \begin{pmatrix} \chi_{+,k} \\ \chi_{-,k} \end{pmatrix} = (\vec{v}_+ \ \vec{v}_-)^\dagger(k) \Psi_k \quad (27)$$

where we introduced orthonormal eigenvectors  $\{\vec{v}_\pm\}$

$$\vec{v}_\pm(k) = \frac{1}{\sqrt{2R(R \mp R_3)}} \begin{pmatrix} R_1 - iR_2 \\ \pm R - R_3 \end{pmatrix}. \quad (28)$$

Thus, the ground state of SSH Hamiltonian is

$$|\Omega\rangle = \prod_k \chi_{-,k}^\dagger |0\rangle \quad (29)$$

where  $|0\rangle$  is the Fock vacuum of (25).

On the other hand, (25) consists of three parts – analogues of left- and right-moving continuum Dirac Hamiltonian,

$$H_L = \sum_k R_3 c_k^\dagger c_k, \quad H_R = - \sum_k R_3 d_k^\dagger d_k, \quad (30)$$

and the mass part

$$H_{LR} = \sum_k \Psi_k^\dagger (R_1 \sigma_1 + R_2 \sigma_2) \Psi_k. \quad (31)$$

The ground states of  $H_L$  and  $H_R$ , denoted as  $|G_L\rangle$  and  $|G_R\rangle$ , respectively, are

$$|G_L\rangle = \prod_{k < 0} c_k^\dagger |0\rangle_L, \quad |G_R\rangle = \prod_{k > 0} d_k^\dagger |0\rangle_R. \quad (32)$$

where  $|0\rangle_{L,R}$  are the Fock vacuum of  $H_{L,R}$ , respectively. It is not hard to see (27) is a Bogoliubov transformation from the creation and annihilation operators of  $H_L + H_R$  in (30) and  $H$  in (25). Therefore the (unnormalized) ground state  $|\Omega\rangle$  defined in (29) can be expressed in terms of  $|G_L\rangle$  and  $|G_R\rangle$  as

$$|\Omega\rangle = \exp \left[ - \sum_{k > 0} \left( \frac{v_k}{u_k} c_k^\dagger d_k + \frac{u_{-k}}{v_{-k}} d_{-k}^\dagger c_{-k} \right) \right] |G_L\rangle \otimes |G_R\rangle, \quad (33)$$

where

$$\begin{pmatrix} u_k \\ v_k \end{pmatrix} = \frac{1}{\sqrt{2R(R + R_3)}} \begin{pmatrix} R + R_3 \\ R_1 - iR_2 \end{pmatrix}. \quad (34)$$

We then introduce the  $SU(2)$  algebra generators  $J_0^{(k)}$ ,  $J_\pm^{(k)}$  (and similarly  $J_0^{(-k)}$ ,  $J_\pm^{(-k)}$ ) in terms of the fermion creation and annihilation operators

$$J_+^{(k)} = -i c_k^\dagger d_k, \quad J_-^{(k)} = i d_k^\dagger c_k, \quad (35)$$

$$J_0^{(k)} = \frac{1}{2} (c_k^\dagger c_k - d_k^\dagger d_k),$$

$$J_+^{(-k)} = i c_{-k}^\dagger d_{-k}, \quad J_-^{(-k)} = -i d_{-k}^\dagger c_{-k},$$

$$J_0^{(-k)} = \frac{1}{2} (c_{-k}^\dagger c_{-k} - d_{-k}^\dagger d_{-k}), \quad (36)$$

where  $k > 0$ . Thus, the ground state (29) can be rewritten in terms of  $SU(2)$  coherent states

$$|\Omega\rangle = \prod_{k > 0} \cos^2 \frac{\phi_k}{2} e^{-i \tan \frac{\phi_k}{2} (e^{-i\psi_k} J_+^{(k)} + e^{i\psi_k} J_+^{(-k)})} \bigotimes_{k \in \text{BZ}} |1/2; -1/2\rangle_k. \quad (37)$$

Finally, the Hamiltonian of SSH model can be rewritten in terms of  $SU(2)$  algebra generators as

$$H = \sum_{k > 0} R \left[ 2 \cos \phi_k \left( J_0^{(k)} + J_0^{(-k)} \right) + i \sin \phi_k \left( e^{-i\psi_k} J_+^{(k)} + e^{i\psi_k} J_+^{(-k)} \right) - i \sin \phi_k \left( e^{i\psi_k} J_-^{(k)} + e^{-i\psi_k} J_-^{(-k)} \right) \right]. \quad (38)$$

Above we have used spherical coordinates to rewrite  $\vec{R}(k)$ , in particular,

$$\sin \phi_k \cos \psi_k = \frac{R_1}{R},$$

$$\sin \phi_k \sin \psi_k = \frac{R_2}{R},$$

$$\cos \phi_k = \frac{R_3}{R}. \quad (39)$$

In the main text we have worked with  $\mu_s = 0$  that corresponds to  $R_2 = \psi_k = 0$  in these expressions.

## Appendix B: $SU(2)$ coherent states

To make this article self-contained, we collect some of the tools from  $SU(2)$  coherent states that were used in the main text (see more in e.g. [46, 47]). We start with  $SU(2)$  algebra  $[J_i, J_j] = i\epsilon_{ijk}J_k$ , expressed in terms of the ladder operators  $J_{\pm} = J_1 \pm iJ_2$  and  $J_0 = J_3$  as

$$[J_+, J_-] = 2J_0, \quad [J_0, J_{\pm}] = \pm J_{\pm}. \quad (40)$$

The relevant coherent states are defined by action of a displacement operator on the lowest-weight state  $|j, -j\rangle$  (i.e.,  $J_- |j, -j\rangle = 0$ ) labeled by (half or) integer  $j$

$$|z, j\rangle = e^{\xi J_+ - \bar{\xi} J_-} |j, -j\rangle = e^{z J_+} e^{\ln(1+z\bar{z}) J_0} e^{-\bar{z} J_-} |j, -j\rangle. \quad (41)$$

In the above we defined complex parameter

$$\xi = \frac{\theta}{2} e^{-i\varphi}, \quad 0 \leq \theta < \pi, \quad 0 \leq \varphi \leq 2\pi, \quad (42)$$

with its complex conjugate  $\bar{\xi}$  as well as

$$z = \tan\left(\frac{\theta}{2}\right) e^{-i\varphi}, \quad (43)$$

with complex conjugate  $\bar{z}$ .

These coherent states are employed in the Krylov/spread complexity context when we e.g. chose  $\xi = -is\frac{\phi}{2}$ , so  $\theta = s\phi$  and  $\varphi = \pi/2$ , such that the state becomes

$$|z, j\rangle = e^{-is\frac{\phi}{2}(J_+ + J_-)} |j, -j\rangle = \sum_{n=0}^{2j} \psi_n(s) |K_n\rangle, \quad (44)$$

where

$$\psi_n(s) = \frac{(-i)^n \tan^n\left(\frac{s\phi}{2}\right)}{\left(\cos\frac{s\phi}{2}\right)^{-2j}} \sqrt{\frac{\Gamma(2j+1)}{n!\Gamma(2j-n+1)}}, \quad (45)$$

and Krylov basis vectors are

$$|K_n\rangle = |j, -j+n\rangle = \sqrt{\frac{\Gamma(2j-n+1)}{n!\Gamma(2j+1)}} J_+^n |j, -j\rangle. \quad (46)$$

The amplitude (45) satisfies a discrete Schrodinger equation (5) with  $a_n = 0$  and  $2j+1$  coefficients

$$b_n = \frac{\phi}{2} \sqrt{n(2j-n+1)}, \quad n = 0, \dots, 2j. \quad (47)$$

The Krylov or spread complexity in this case becomes

$$\mathcal{C}(s) = \sum_n n |\psi_n(s)|^2 = 2j \sin^2\left(\frac{s\phi}{2}\right). \quad (48)$$

In the main text, we only needed these results for the  $j = 1/2$  representation where

$$\mathcal{C}(s) = |\Psi_1(s)|^2 = \sin^2\left(\frac{s\phi}{2}\right). \quad (49)$$

More generally, we may consider time evolution

$$|\Psi(t)\rangle = e^{-iHt} |j, -j\rangle, \quad (50)$$

with coherence preserving Hamiltonian

$$H = \gamma J_0 + \alpha(J_+ + J_-). \quad (51)$$

Then the state can be written as

$$|\Psi(t)\rangle = \sum_{n=0}^{2j} \Psi_n(t) |K_n\rangle, \quad (52)$$

with Krylov basis vectors (46) and coefficients

$$\Psi_n(t) = e^{-jB} A^n \sqrt{\frac{\Gamma(2j+1)}{n!\Gamma(2j-n+1)}}, \quad (53)$$

where

$$A = \frac{1}{i\sqrt{1 + \frac{\gamma^2}{4\alpha^2}} \cot\left(\alpha t \sqrt{1 + \frac{\gamma^2}{4\alpha^2}}\right) - \frac{\gamma}{2\alpha}}, \quad (54)$$

$$e^{-jB} = \left( \cos\left(\alpha t \sqrt{1 + \frac{\gamma^2}{4\alpha^2}}\right) + \frac{i\gamma}{2\alpha\sqrt{1 + \frac{\gamma^2}{4\alpha^2}}} \sin\left(\alpha t \sqrt{1 + \frac{\gamma^2}{4\alpha^2}}\right) \right)^{2j}. \quad (55)$$

Coefficients  $\Psi_n(t)$  in (53) are solutions of the Schrodinger equation (5) with Lanczos coefficients

$$a_n = \gamma(-j+n), \quad b_n = \alpha\sqrt{n(2j-n+1)}. \quad (56)$$

Finally, the complexity becomes

$$\mathcal{C}(t) = \sum_n n |\Psi_n(t)|^2 = \frac{2j}{1 + \frac{\gamma^2}{4\alpha^2}} \sin^2\left(\alpha t \sqrt{1 + \frac{\gamma^2}{4\alpha^2}}\right). \quad (57)$$

For the quench, we will also needed the following return amplitude

$$S(t) = \langle j, -j | D^\dagger(z_i) e^{iH_f t} D(z_i) |j, -j\rangle \quad (58)$$

where the  $SU(2)$  displacement operator is

$$D(z_i) = e^{-i\frac{\phi_i}{2}(J_+ + J_-)}, \quad (59)$$

and a Hamiltonian  $H_f$  has a form (51) with  $\gamma = 2R_3$  and  $\alpha = iR_1$ .

Generally, using the BCH relation we derive

$$S(t) = (\cos(R_f t) - i \cos(\phi_f - \phi_i) \sin(R_f t))^{2j}. \quad (60)$$

For  $j = 1/2$ , the moments of this return amplitude are

$$\mu_n = R_f^n \left( \cos\frac{\pi n}{2} - i \cos(\phi_f - \phi_i) \sin\frac{\pi n}{2} \right), \quad (61)$$

and they correspond to the two Lanczos coefficients

$$\begin{aligned} a_0 &= -R_f \cos(\phi_f - \phi_i), & a_1 &= R_f \cos(\phi_f - \phi_i), \\ b_1 &= R_f |\sin(\phi_f - \phi_i)|, \end{aligned} \quad (62)$$

while all the higher ones vanishing. This again allowed us to map our state expanded in the Krylov basis to  $SU(2)$  coherent state

$$|\Psi(t)\rangle = e^{-iH_t t} |\Omega_i\rangle = \sum_{n=0}^1 \psi_n(t) |K_n\rangle, \quad (63)$$

where

$$\psi_0(t) = S(t)^*, \quad \psi_1(t) = -i |\sin(\phi_f - \phi_i)| \sin(R_f t), \quad (64)$$

and the two basis vectors  $|K_0\rangle = |1/2, -1/2\rangle$ ,  $|K_1\rangle = |1/2, 1/2\rangle$ . This leads to the spread complexity per mode (19).

Finally, observe that for  $j = 1/2$  representations of  $SU(2)$ , since we only have two complex amplitudes  $\Psi_0(t)$  and  $\Psi_1(t)$ , we can relate the spread complexity  $\mathcal{C}(t) = |\psi_1(t)|^2$  to the return amplitude  $S(t) = \psi_0(t)$ . Indeed, by unitarity, probabilities sum up to identity and we have

$$|\Psi_0|^2 + |\Psi_1|^2 = 1 \leftrightarrow \mathcal{C}(t) = 1 - |S(t)|^2. \quad (65)$$

This simple relation will not hold for a more general time evolution that requires higher number of Krylov basis vectors. Nevertheless, understanding the relation between spread complexity and Loschmidt echo is an interesting future problem. We thank Diptarka Das for pointing this to us.

### Appendix C: Early and late times

This appendix contains more details on universal behaviours of the evolution of complexity in the early and late times. Firstly, at the early times, after of the quench, i.e.,  $t \sim 0^+$ , the time evolution of complexity (20) becomes

$$\mathcal{C}(t \sim 0) \simeq t^2 \times \int_0^\pi \frac{dk}{\pi} \frac{(t_1^f t_2^i - t_1^i t_2^f)^2 \sin^2(k)}{R_i^2}. \quad (66)$$

In terms of the ratios of  $t_2^{i,f}/t_1^{i,f}$ , denoted as  $\alpha$  and  $\beta$  for initial and final parameters, respectively, the spread complexity is

$$\begin{aligned} \mathcal{C}(t \sim 0) &= (t t_1^f)^2 (\alpha - \beta)^2 \frac{(|1 + \alpha| - |1 - \alpha|)^2}{8\alpha^2} \\ &= t^2 (t_1^f t_2^i - t_1^i t_2^f)^2 \frac{(t_1^i + t_2^i - |t_1^i - t_2^i|)^2}{8 (t_1^i t_2^i)^2}. \end{aligned} \quad (67)$$

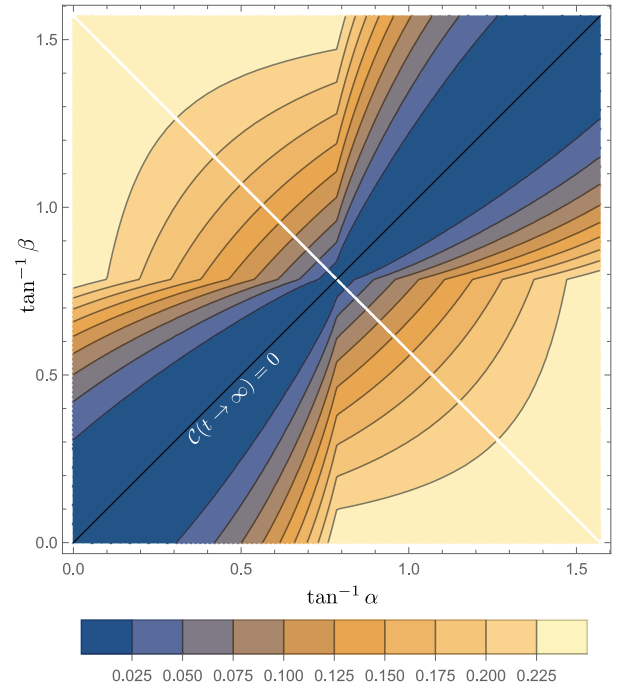


FIG. 3. Spread complexity constant at late times  $\mathcal{C}(t \rightarrow \infty; \alpha, \beta)$ , shown in (23).

On the other hand, for late times, i.e.,  $t \rightarrow \infty$ , we notice that the time evolution of (20) can be estimated as follows. First, (20) is equivalent to

$$\mathcal{C}(t) = 2 \int_0^\pi \frac{dk}{2\pi} \frac{(t_1^f t_2^i - t_1^i t_2^f)^2 \sin^2(k)}{R_f^2 R_i^2} \times \frac{1 - \cos 2R_f t}{2}. \quad (68)$$

We can then change the integration variable in the second term such that

$$\begin{aligned} &\int_0^\pi \frac{dk}{2\pi} \frac{(t_1^f t_2^i - t_1^i t_2^f)^2 \sin^2(k)}{R_f^2 R_i^2} \cos 2R_f t \\ &= \frac{(t_1^f t_2^i - t_1^i t_2^f)^2}{t_1^f t_2^f} \int_{k(R_f) \in (0, \pi)} \frac{dR_f}{2\pi} \frac{\sin k(R_f)}{R_f \cdot R_i^2(R_f)} \cos 2R_f t. \end{aligned} \quad (69)$$

Now, because for  $t \rightarrow \infty$  the cosine function is highly oscillating in the interval  $(0, |t_{1,f} \pm t_{2,f}|]$ , where the integral range belongs to, this integral is always negligible, no matter what the concrete form of  $\frac{\sin k(R_f)}{R_f \cdot R_i^2(R_f)}$  in terms of  $R_f$  is. This way we find the late time constant as

$$\mathcal{C}(t \rightarrow \infty) \simeq \int_0^\pi \frac{dk}{2\pi} \frac{(t_1^f t_2^i - t_1^i t_2^f)^2 \sin^2(k)}{R_f^2 R_i^2}. \quad (70)$$

This is also equivalent to replacing the time dependent factor  $\sin^2(R_f t)$  by  $1/2$ . This expression integrates to

(23) and is plotted in Fig. 3. Note that naively, (23) is singular for  $\alpha\beta = 1$  (the white diagonal on Fig. 3),

$\alpha = 0$  and  $\beta = 0$ . These cases should be analyzed more carefully starting from (20) with these values of  $\alpha$  and  $\beta$  and only then performing the integral over momenta.